

Catalysis Science & Technology

Accepted Manuscript



This article can be cited before page numbers have been issued, to do this please use: L. HDIDOU, K. khallouk, B. Manoun, A. Solhy, A. OUKARROUM and A. Barakat, *Catal. Sci. Technol.*, 2018, DOI: 10.1039/C8CY00576A.



This is an Accepted Manuscript, which has been through the Royal Society of Chemistry peer review process and has been accepted for publication.

Accepted Manuscripts are published online shortly after acceptance, before technical editing, formatting and proof reading. Using this free service, authors can make their results available to the community, in citable form, before we publish the edited article. We will replace this Accepted Manuscript with the edited and formatted Advance Article as soon as it is available.

You can find more information about Accepted Manuscripts in the [author guidelines](#).

Please note that technical editing may introduce minor changes to the text and/or graphics, which may alter content. The journal's standard [Terms & Conditions](#) and the ethical guidelines, outlined in our [author and reviewer resource centre](#), still apply. In no event shall the Royal Society of Chemistry be held responsible for any errors or omissions in this Accepted Manuscript or any consequences arising from the use of any information it contains.



Journal Name

ARTICLE

Synthesis of CoFeO Mixed Oxide via Alginate Gelation Process as an Efficient Heterogeneous Catalyst for Lignin Depolymerization in Water

L. Hdidou,^{a,b} K. Khallouk,^{c,d} A. Solhy,^a B. Manoun,^{a,e} A. Ouarrour,^a and A. Barakat^{a,c*}

Received 00th January 20xx,
Accepted 00th January 20xx

DOI: 10.1039/x0xx00000x

www.rsc.org/

The catalytic oxidative fragmentation of dimer and lignin polymer extracted from wheat straw was successfully performed under eco-friendly conditions: 10%O₂/N₂ as oxidizing agent, water as solvent (pH ≈ 7), Co₃O₄, Fe₂O₃ and CoFeO mixed oxides as heterogeneous catalysts, and at temperatures towards: T = 150°C and 200 °C. These catalysts showed unexpectedly tunable selectivity that directly depends on the composition of the selected bimetallic nanoparticles. High selectivity for benzoic acid and alkylbenzene (above 50%) was observed over Co₅₀-Fe₅₀ at 200°C. Under similar conditions the conversion of wheat organosolv lignin over Co₅₀-Fe₅₀ at 150°C for 4 hrs yielded up to 50 wt% of monomeric species (based on dry lignin) and up to 19% of aromatic molecules with high selectivity to aromatic aldehyde (Syringaldehyde and Vanillin) up to 60%. An important fraction of water-soluble oligomers, with low molecular weights, was also formed during the catalytic treatment. The nanomaterials oxides were readily separated from lignin residual during the recyclability test. The yield and the product distribution can be tuned by choosing the oxidation parameters: temperature, reaction time, oxygen partial pressure, solvent and catalyst charges.

Introduction

Lignin, that is a major component of plants, is one of the most abundant sources of organic carbon on the planet. It is a cross-linked polyphenolic material, with complex, irregular and very stable structure, and therefore difficult to convert into monomeric products. Consequently, more than 95 wt% of the lignin production (estimated at over 70 million tons/year) is used for the generation of heat and power, and only a small amount is converted into chemicals of industrial interest^{1, 2}. Nowadays, with declining fossil sources, the lignin is recognized as a suitable renewable raw material for production of transport fuels^{3, 4}, materials^{5, 6} and chemicals^{2, 7}. Lignin could be processed into commercial products via either biological or thermochemical processes. Among the chemical processes used for the valorization of this natural polymer, oxidative degradation to useful low molecular weight seems to be very promising. It is worth noting that the oxidation of lignins to aromatic aldehydes such as vanillin, syringaldehyde and p-hydroxybenzaldehyde has been much studied and is commercially important⁸⁻¹⁰. Different systems and methods were used for the lignin oxidative degradation among which we mention: air in alkaline solution at high temperatures⁷, nitro aromatics^{11, 12}, electrochemical oxidation^{13, 14} and combined nitro aromatic/electrochemical oxidation¹⁵. More recently, the catalytic oxidation with oxygen and hydrogen peroxide was suggested as an efficient method for lignin degradation in industrial pulping

technologies such as delignification/bleaching, effluents treatment and aromatic compounds fabrication. Many homogeneous and heterogeneous catalysts have been used for the oxidation of both lignin and lignin model compounds. For example, lignins have been oxidized under alkaline conditions, in the presence of Pd/γ-Al₂O₃¹⁶ or copper (II) and cobalt (II) salts as catalysts^{17, 18} to give aromatic aldehydes. The polyoxometalates have been used as multifunctional catalysts in the conversion of kraft lignin into monomeric products¹⁹ or for the delignification of lignocellulosic pulps²⁰⁻²³. The aerobic oxidative cleavage of lignins was effectively performed with metal/bromide catalysts in acetic acid²⁴⁻²⁶. Recently, a perovskite-type oxide has been proposed as heterogeneous catalyst for the alkaline oxidation of lignin to aromatic aldehyde⁷. Crestini *et al.* studied the ability of the hydrogen peroxide as oxidant for the lignin degradation, using catalytic systems based on methyltrioxorhenium²⁷ or porphyrins²⁸. Most of catalytic oxidation studies were performed in acidic or alkaline aqueous media or in organic solvents. With respect to the green chemistry principles, the ideal oxidation system should use oxygen as an oxidant, stable solids as heterogeneous catalysts and water as a solvent^{29,30}.

In view of these findings, in this study we developed an effective method for the oxidative depolymerization of lignin model compounds, using molecular oxygen, metallic oxides as heterogeneous catalysts, and water at pH = 7 as solvent. The screening of Fe-Co catalysts, with outstanding textural properties, based on lignin model depolymerization was prepared by an original method. In this study, we report also for the first time on the oxidative fragmentation and depolymerization of extracted lignin polymer, performed under eco-friendly conditions (water, 150 °C, 10 bar, 4 h). Organosolv lignin was oxidized with oxygen in the presence of Co-Fe mixed oxides as heterogeneous catalysts.

Experimental section

^a Mohammed VI Polytechnic University (UM6P). Benguerir, Maroc

^b LIMAT, FSBM, Hassan II University, Maroc

^c IATE, CIRAD, Montpellier SupAgro, INRA, Université de Montpellier, France

^d LCME, EST, Université Sidi Mohammed Ben Abdellah, 30000, Fès, Maroc.

^e LS3M, Polydisciplinary Faculty of Khouribga, Hassan I University, Maroc

ARTICLE

Journal Name

Starting materials

Organosolv lignin: The Organosolv lignin was extracted from wheat straw according to a procedure described previously³¹. The average-molecular weights (evaluated by size-exclusion chromatography) was 3180 g/mol for the Organosolv lignin.

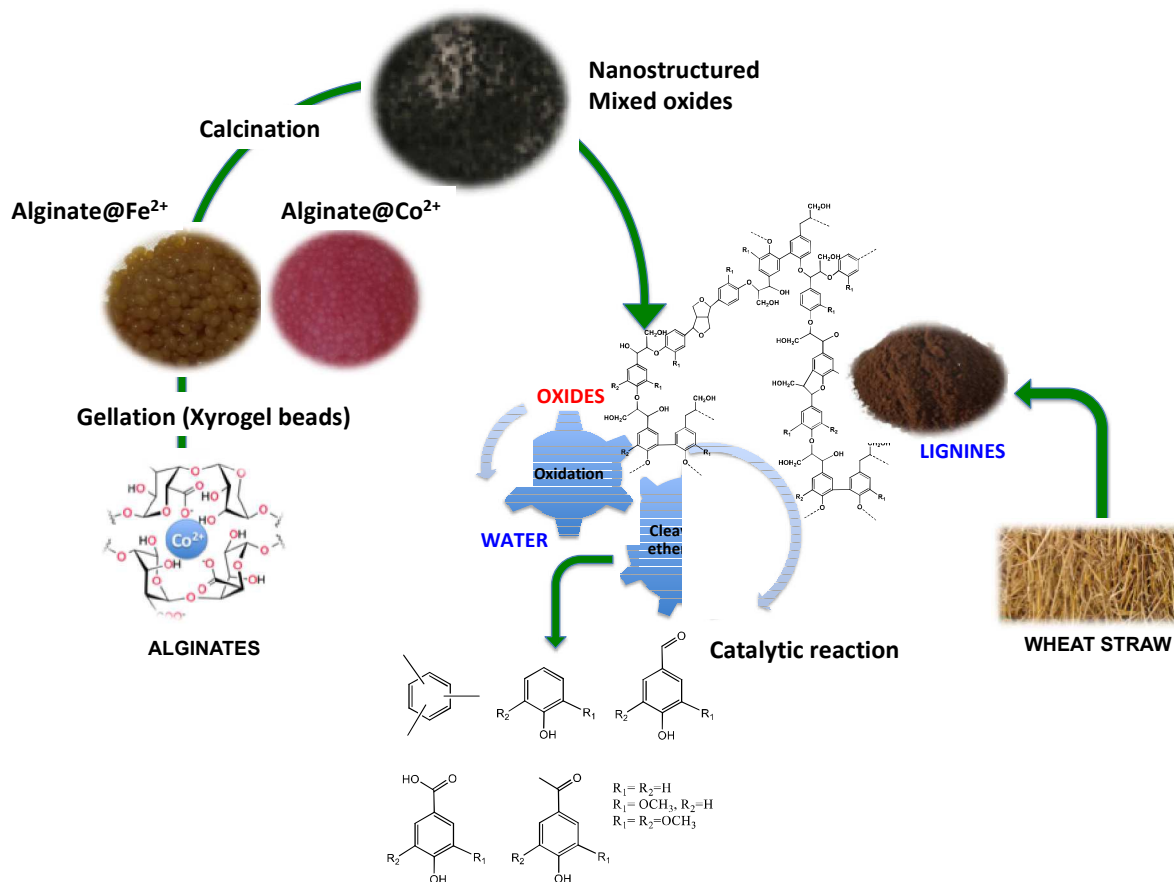


Fig.1: Iron-Cobalt oxide nanomaterials synthesis and oxidative catalytic depolymerisation of lignin developed in this study

Lignin model compound synthesis:

4-(benzyloxy)-3-methoxybenzaldehyde lignin model was synthesized according to Fig.S1. 4g of vanillin was dissolved in 20ml of pyridine at 5°C. 3 cm³ of benzoyl chloride was added under magnetic stirring. After 30 min, 50 cm³ of hexane was injected to the reaction mixture. The precipitate was filtered and crystallised from ethyl acetate and hexane, to give 4-(benzyloxy)-3-methoxybenzaldehyde in 92%.

Characterization of lignin

Thioacidolysis: Lignin polymer was degraded by thioacidolysis to estimate the nature of the aromatic units, according to reference³².

Size-exclusion chromatography of acetylated samples in THF: The molecular-mass distribution of the initial and residual lignin has been analyzed using size-exclusion chromatography (SEC). Prior to chromatography, the lignin was submitted to acetylation in a mixture of acetic anhydride-pyridine (1:1) for 24 h at 40°C. The SEC

analysis was performed using a multi-detection system consisting of a pump (model 510, Waters), autosampler (U6K injector, Waters), two Polymer Laboratories (PLgel Mixed D, 5μ) column and UV-detector (model 920, Waters). Separation in THF was performed by injecting 100 μL of 0.1 % of acetylated samples into thermostatically controlled PLgel columns (40°C). The flow rate was 1 ml/min. Molar mass evaluation was based on elution polystyrene standards^{32,33}.

Cobalt-Iron oxide preparation and characterization

Cobalt-iron oxides with different Co/Fe ratios were prepared via alginate gelling method. 2wt% sodium alginate aqueous solution was prepared under a medium stirring at room temperature for around 3h. 60 ml of the obtained solution was added dropwise into a 100 ml of homogeneous metal solution containing Co²⁺, Fe³⁺, Fe²⁺ and/or a mixture of Co²⁺/Fe²⁺ with a total concentration of 0.15M. The obtained hydrogel beads were left in the metal solution overnight with a gentle stirring. The beads were then removed from the solution, filtered and washed with distilled water three times to remove the adsorbed free cation in the surface of alginate beads. Alginates@cations (Fe²⁺ and Co²⁺) were then dried at 40°C giving

xerogel beads. Alginates@ cations xerogel beads were also calcinated at 550°C for 4h giving nanostructured oxides (Fig.1).

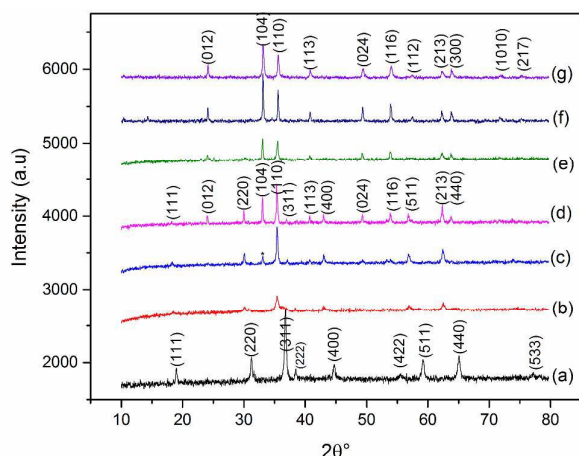


Fig.3: X-ray patterns of the synthesized oxides: (a) Co_3O_4 , (b) $\text{Co}_{2.4}\text{Fe}_{0.6}\text{O}_4$, (c) $\text{Co}_{1.8}\text{Fe}_{1.2}\text{O}_4$, (d) $\text{Co}_{0.8}\text{Fe}_{1.2}\text{O}_3/\text{Co}_{1.8}\text{Fe}_{1.2}\text{O}_4$, (e) $\text{Co}_{0.8}\text{Fe}_{1.2}\text{O}_3$, (f) $\text{Co}_{0.4}\text{Fe}_{1.6}\text{O}_3$ and (g) $\alpha\text{-Fe}_2\text{O}_3$

The phase of the various samples were determined by powder X-ray diffraction, using a Bruker D2 PHASER diffractometer, with the Bragg-Brentano geometry, using $\text{CuK}\alpha$ radiation ($\lambda=1.5418 \text{ \AA}$) with 30KV and 10 mA. The pattern was scanned through steps of 0.010142° (2θ), between 10 and 80° . The morphology and the size were observed by scanning electron microscopy SEM. The SEM was coupled to an Energy Dispersive X-ray Spectroscopy EDS that give us a chemical analysis of the materials surface.

Catalytic depolymerisation of dimer and lignin polymer

Experiments were conducted in a reactor of 500 cm^3 (PARR 5500, USA). The reactor was loaded with 50 mg of dimer and polymer lignin, 10 or 20 mg of catalyst, 30 mL of distilled water and O_2 (10% in N_2) (100 and 200KPa). The mixture was heated for 2 or 4h at 150°C or 200°C , and then the mixture was extracted with CH_2Cl_2 (Fig.2). The organic solution was dried over MgSO_4 and evaporated under reduced pressure. The residues were dissolved in 1mL of CH_2Cl_2 in the presence of internal standard GC-MS analyzed. For the residue (insoluble fraction in CH_2Cl_2), water was removed and the solid residue was dissolved in dioxane (30mL) and filtered to eliminate the catalyst. The dioxane was evaporated under reduced pressure at 50°C and the residue was dissolved in dioxane (3 mL) and freeze dried. The organic extract was dried under anhydrous magnesium sulphate and concentrated at 40°C , using a rotating evaporator. The analysis of the organic phase was performed on a system GC/MS-QP 2010 Shimadzu, equipped with a SLB-5MS capillary column ($30 \text{ m} \times 0.25 \text{ mm} \times 0.25 \mu\text{m}$), using helium as a carrier gas. The temperature was ramped at $10^\circ\text{C}/\text{min}$ from 80 to 250°C , where it was kept for 10 min.

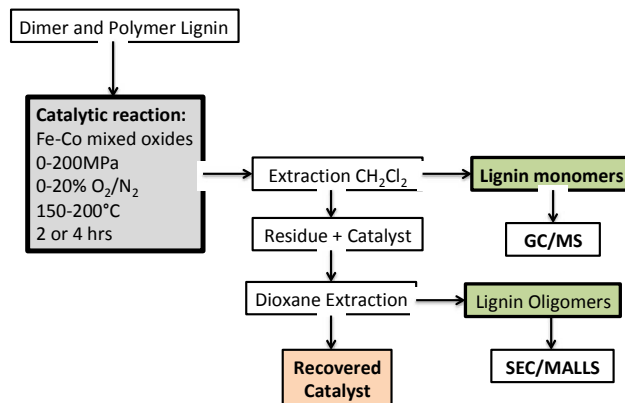


Fig.2: Experimental process of Catalytic depolymerization of dimer and lignin polymer

Results

Characterization of Cobalt-Iron oxides nanomaterials

The composition of metallic oxides depending on Co/Fe atom ratios in the gelling solution of alginates polymer. The coordination between Co^{2+} , Fe^{3+} , Fe^{2+} and the alginate functional groups (OH , COOH) provide nano-oxides nucleation and growth sites (Fig.1). After the calcination step, the organic matter degrades releasing the metal oxides nanoparticles. The oxide phases obtained depend essentially on the Co/Fe atom ratios (Fig.3). Due to the thermal treatment of alginate@ Co^{2+} and alginate@ Fe^{2+} xerogels, pure cubic spinel Co_3O_4 (Co_{100}) (Fig.3-a) and hematite $\alpha\text{-Fe}_2\text{O}_3$ (Fe_{100}) (Fig.3-g) were produced. From XRD patterns (Fig.3-a) the peaks at 2θ values $19.0, 31.2, 36.7, 38.4, 44.8, 55.6, 59.2, 65.0$ correspond to the diffraction planes (111), (220), (311), (222), (400), (422), (511), (440). This phase is assigned to Co_3O_4 face-centred cubic structure belonging to Fd-3m space group. The insertion of iron ions in tetrahedral and octahedral sites allows the formation of cobalt ferrite oxides $\text{Co}_{2.4}\text{Fe}_{0.6}\text{O}_4$ ($\text{Co}_{80}\text{-Fe}_{20}$) (Fig.3-b) and $\text{Co}_{1.8}\text{Fe}_{1.2}\text{O}_4$ ($\text{Co}_{60}\text{-Fe}_{40}$) (Fig.3-c); both oxides have the same space group as for Co_3O_4 . When the iron concentration achieved 50% of the total solution concentration a transition zone was observed, both $\text{Co}_{0.8}\text{Fe}_{1.2}\text{O}_3$ and $\text{Co}_{1.8}\text{Fe}_{1.2}\text{O}_4$ ($\text{Co}_{50}\text{-Fe}_{50}$) co-exist (Fig.3-d). (Fig.3-e and -f) refers to $\text{Co}_{0.8}\text{Fe}_{1.2}\text{O}_3$ ($\text{Co}_{40}\text{-Fe}_{60}$) and $\text{Co}_{0.4}\text{Fe}_{1.6}\text{O}_3$ ($\text{Co}_{20}\text{-Fe}_{80}$) respectively, these phases exhibit hexagonal structure whose main crystallographic planes are: (012), (104), (110), (113), (024), (116), (214) and (300). The compounds crystallize in R-3c space group. The large Full Width at Half Maximum and low peak intensities reveal the formation of nanostructured oxides³⁴.

Fig.4 shows the evolution of the unit volume for all samples. The phase transition from cubic to hexagonal is well defined when $\text{Fe}/(\text{Co}+\text{Fe}) = 0.5$. In the case of the Co_3O_4 the substitution of Co^{3+} by Fe^{3+} in both octahedral and tetrahedral sites leads to a slight increase in the lattice parameters and the unit volume since $r(\text{Fe}^{3+}) = 0.55 > r(\text{Co}^{3+}) = 0.545$ ³⁵. Also the incorporation of Co^{2+} in the hematite lattice increases faintly the unit volume because $r(\text{Co}^{2+}) = 0.65 > r(\text{Fe}^{3+}) = 0.55$ ³⁵. These results could be confirmed from the shift of the peaks to lower θ value.

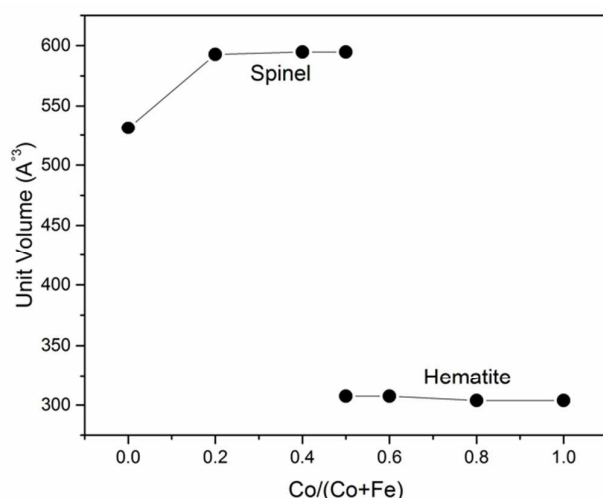


Fig. 4: Unit volume evolution of the as-synthesized $\text{Co}_{3-x}\text{Fe}_x\text{O}_4$, Co: $\alpha\text{-Fe}_2\text{O}_3$ and $\alpha\text{-Fe}_2\text{O}_3$ oxides

The pore structure parameters of oxides catalysts including specific surface area (m^2/g) pore volume (cm^3/g) are shown in (Table 1). A clear effect of Co/Fe atom ratios on S_{BET} and pore volume was observed. A good correlation was observed with particle size and S_{BET} , as we know that particles with smaller size may possess larger S_{BET} . In Table 1, it can be found that the $\text{Co}_{50}\text{-Fe}_{50}$ oxide has a greater porosity and S_{BET} than the $\text{Co}_{50}\text{-Fe}_{50}$ compared to other nanomaterials oxides. Besides, the $\text{Co}_{50}\text{-Fe}_{50}$ oxide comprises a total pore volume ($0.045 \text{ cm}^3/\text{g}$) that is larger than that of the Fe_{100} ($0.07 \text{ cm}^3/\text{g}$) and Co_{100} ($0.07 \text{ cm}^3/\text{g}$). The S_{BET} for the $\text{Co}_{50}\text{-Fe}_{50}$ was calculated as $42.7 \text{ m}^2/\text{g}$ compared to only $31.3 \text{ m}^2/\text{g}$ for Co_{100} , $28.7 \text{ m}^2/\text{g}$ for $\text{Co}_{80}\text{-Fe}_{20}$, $24.4 \text{ m}^2/\text{g}$ for Fe_{100} , and $18.8 \text{ m}^2/\text{g}$ for $\text{Co}_{20}\text{-Fe}_{80}$. The increased pore volume and surface area of $\text{Co}_{50}\text{-Fe}_{50}$ oxide may be attributed to the presence of two phases hematite and spinel resulted by the incorporation of Co^{2+} in the hematite lattice that increased faintly the unit volume. The influence of Co/Fe atom ratios on the morphology and the microstructure of Co-Fe mixed oxides nanoparticles was investigated using SEM, and the images are shown in Fig.5. Co-Fe synthesized oxides showed different morphology and microstructure which depending on the calcination temperature and the Co/Fe atom ratio. Spherical-like particles with an average diameter of 39 nm were observed for Co_{100} (Fig.5-a). The cubic spinel structure must give a cubic morphology owing to the privileged growth along the axes $\langle 100 \rangle$, however this shape exhibit an isotropic evolution providing spherical particles, like this result was reported by Givanneli et al.³⁶. In the case of cobalt ferrite (Fig.5-b) and (Fig.5-c) polyhedral with octahedral-like morphology was formed. The nanoparticles size (NPs) is around 57.3 and 41.8 nm respectively. The formation of the octahedron shape is due to the growth rate along the $\langle 100 \rangle$ directions that is faster than along $\langle 111 \rangle$, that have lowest surface energy^{37, 38}. From (Fig.5- e and -f) ($\text{Co}_{40}\text{-Fe}_{60}$) and ($\text{Co}_{20}\text{-Fe}_{80}$) nanoparticles have a flake-like morphology following the same shape of hematite nano-oxide (Fig.5- f) with a size distribution in the range of 110 to 216 nm and

50.2 to 114 nm respectively. Alginate biopolymer acts as a sacrificial bio-template. All samples were analyzed with energy dispersive X-ray spectroscopy (EDS) to determine their elemental composition. (Table 1) reveals the presence of Co and O elements for Co_{100} nanoparticles, with increasing iron amount cobalt percentage decrease until the pure Fe_{100} where only Fe and O were detected.

Catalyst screening: Oxidative catalytic depolymerization of dimers lignin model

Catalytic oxidation of lignin dimer was performed over different synthesized catalysts (Co_{100} , $\text{Co}_{80}\text{-Fe}_{20}$, $\text{Co}_{50}\text{-Fe}_{50}$, $\text{Co}_{20}\text{-Fe}_{80}$ and Fe_{100}). The performance of these catalysts was compared to $\text{Pd}/\text{Al}_2\text{O}_3$ and O_2 without catalysts as a reference.

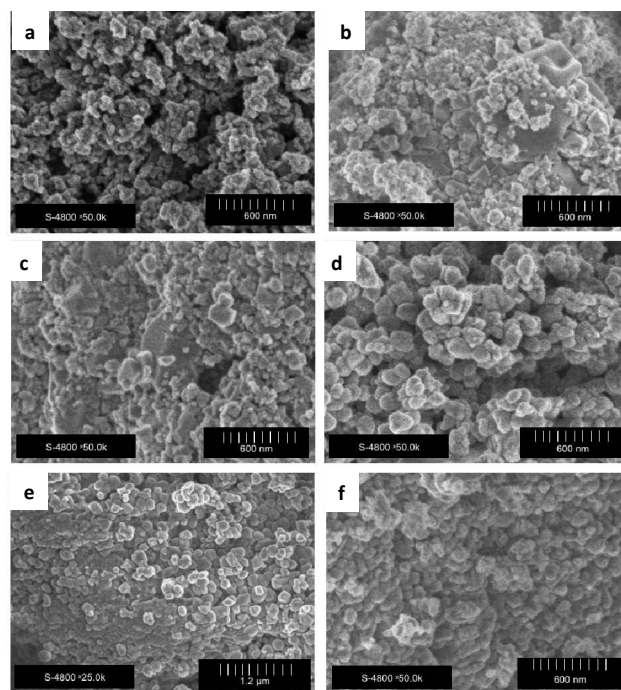
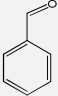
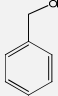
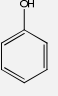
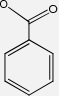
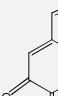
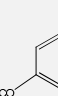
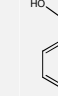


Fig. 5: SEM images of the synthesized oxides: (a) Co_3O_4 , (b) $\text{Co}_{2.4}\text{Fe}_{0.6}\text{O}_4$, (c) $\text{Co}_{1.8}\text{Fe}_{1.2}\text{O}_4$, (d) $\text{Co}_{0.8}\text{Fe}_{1.2}\text{O}_3/\text{Co}_{1.8}\text{Fe}_{1.2}\text{O}_4$, (e) $\text{Co}_{0.8}\text{Fe}_{1.2}\text{O}_3$ and (f) $\alpha\text{-Fe}_2\text{O}_3$.

Journal Name

ARTICLE

Table 1: Nanostructured metal oxides properties							
Catalysts	DRX	SEM	EDX		BET		
	Phase and structure	Morphology	Size (nm)	%Co	%Fe	Surface m ² /g	Pore Vol. cm ³ g ⁻¹
Fe ₁₀₀	Hexagonal Hematite	Flake-like	91	0	31.7 ± 4.0	24.4	0.021
Co ₂₀ -Fe ₈₀	Hexagonal Hematite	Flake-like	157.5	2.0 ± 1.7	29.1 ± 4.4	18.8	0.011
Co ₅₀ -Fe ₅₀	Hexagonal Hematite/ Cubic Spinel	–	31.6	6.9 ± 1.6	24.1 ± 2.4	42.7	0.045
Co ₈₀ -Fe ₂₀	Cubic Spinel	Octahedral-like	57.3	16.4 ± 2.6	20.7 ± 2.3	28.7	0.019
Co ₁₀₀	Cubic Spinel	Spherical-like	39.0	37.5 ± 2,2	0	31.3	0.033

Table 2: Selectivity of major products resulted from catalytic oxidation of lignin dimer over different catalysts in water (pH=7), 100MPa of O ₂							
Catalysts	Selectivity of the products (%)						
							
10%Pd-Al ₂ O ₃	28.0	7.80	0.80	22.4	29.2	8.23	0.00
Co ₁₀₀	38.0	17.4	2.80	19.6	18.7	3.35	0.00
Co ₈₀ -Fe ₂₀	31.2	29.2	0.30	2.20	0.30	36.6	0.00
Co ₅₀ -Fe ₅₀	2.90	4.8	1.30	82.5	0.50	4.70	3.30
Co ₈₀ -Fe ₂₀	27.7	37.4	0.00	1.62	0.00	33.2	0.00
Fe ₁₀₀	17.0	47.6	0.00	2.00	1.50	32.0	0.00
Co ₁₀₀ without O ₂	7.40	50.8	0.00	0.70	0.00	41.2	0.00
O ₂ without cata.	14.3	27.9	0.00	2.90	0.00	54.8	0.00

The mixed oxide Co_{1.8}Fe_{1.2}O₄/ Co_{0.8}Fe_{1.2}O₃ (Co₅₀-Fe₅₀) and Co₃O₄ (Co₁₀₀) showed the highest conversion for lignin dimer 96.9%, and 96.7%, respectively compared to 88.8% obtained over (Fig.6). 10%Pd/Al₂O₃. These results indicate that the combination of heterogeneous catalyst with O₂ oxidant greatly improved dimer depolymerization and functional monomers production. In order to investigate this synergistic, the effect of Co₁₀₀ in the absence of O₂ and O₂ without catalyst has been tested. Fig.6 shows that the conversion is estimated to 54.9% and 52.7%, respectively for Co₁₀₀ in the absence of O₂ and O₂ without catalyst under the same conditions. The higher conversion obtained with Co_{1.8}Fe_{1.2}O₄/ Co_{0.8}Fe_{1.2}O₃ compared to 10%Pd/Al₂O₃ is generally considered as a benchmark material for lignin depolymerisation. Fig.7 show the proposed mechanism of lignin dimer depolymerization, O₂ could be the main responsible of the first ether bond R-O-R' cleavage giving vanillin and benzalcohol products. Nevertheless, the other compounds are formed due to the oxidation reaction with the presence of different catalysts.

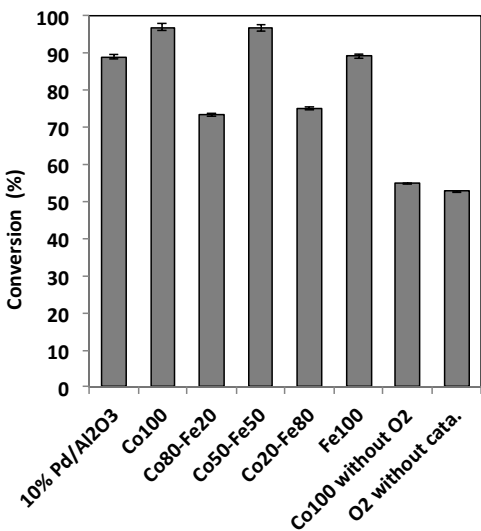


Fig.6: Lignin dimer conversion with different catalyst

ARTICLE

Journal Name

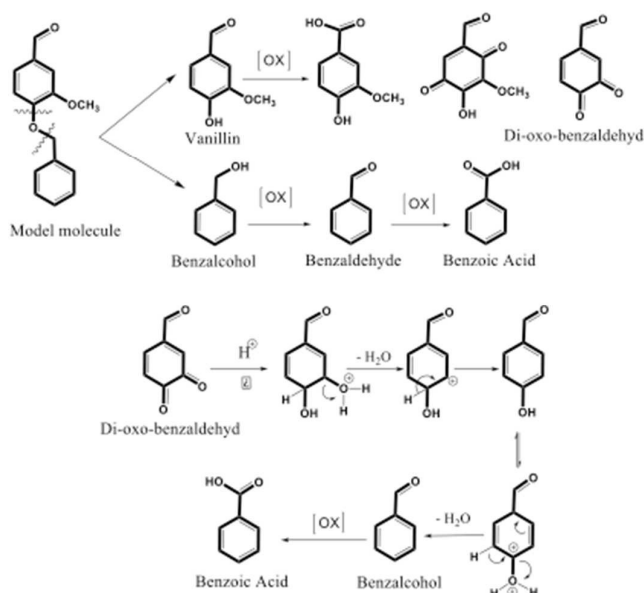


Fig.7: Proposed catalytic depolymerization and oxidation mechanism of lignin dimer.

Re-polymerization and self-condensation ability of reactive radicals formed during lignin oxidation are one of the main faced issues³⁹. However, the catalysts basic sites may inhibit the re-condensation of this phenolic intermediates³⁹. The main products produced *via* dimer lignin model depolymerization are: benzaldehyde, benzalcohol, benzoic acid, and vanillin. The selectivity for each compound depends essentially of the catalyst structures. The use of Co₅₀-Fe₅₀ mixed oxides promotes benzoic acid formation with a high selectivity of 82.5%. This compound may be produced from di-oxo-benzaldehyde (Fig.7) or benzalcohol in which hydroxymethyl group reacts with O₂ to form benzaldehyde that its aldehyde group oxidizes giving carboxylic group. Co₁₀₀ has a moderate selectivity 38%, 17.4%, 19.6%, 18.7% toward benzaldehyde, benzalcohol, Benzoic acid and di-oxo-benzaldehyde, respectively. While Fe₁₀₀ shows a good selectivity for benzalcohol and vanillin. This difference in term of selectivity is directly related to oxides phases, specific surface area and volume pore.

Oxidative catalytic depolymerization of organosolv lignin polymer

The results of catalytic depolymerization of dimer lignin model over Fe-Co oxides indicates clearly that Fe₅₀-Co₅₀ mixed oxide found to be excellent heterogeneous catalysts for the oxidative fragmentation of lignin polymer, with diluted oxygen, under relatively low pressure. Therefore, in this part, catalytic oxidative fragmentation and depolymerization of extracted lignin polymer was performed under similar eco-friendly conditions. Fe₅₀-Co₅₀ catalyst was used in different experiments to convert organosolv lignin in water at 200°C for 4h in the presence of 10% of oxygen (Table 3, Exp. 1). The oligomers (denoted as residual lignin) represented an important fraction of the oxidation products (Fig.8). It is important to note that lignin oligomers with low molecular weight, was completely soluble in the reaction medium. The effect of the reaction time (2h or 4h) and temperature (150°C or 200°C), catalyst charge (Table 3, Exp.5 & 6) was also investigated in the oxidation of extracted wheat straw lignin polymer, in the presence of Fe₅₀-Co₅₀ catalyst for 4h (Table 3, Exp. 1 & 3). The effect of organic solvent by addition of 500 µl of methanol was tested also in the depolymerization of lignin

polymer at 200°C for 4h in the presence of 10% of oxygen (Exp. 2). The results of these six reactions experiments are shown in (Table 3). The distribution of major products identified in GC/MS for different reactions is reported in (Table 3) and (Fig.8). The recovery of lignin monomers was calculated from the aromatic identified compounds using an internal standards, as well as the mass balance was calculated by weighing of the residue after filtration and separation of liquid/solid (Fig.8) and (Table 3), shown that, the lignin conversion and selectivity to different molecules strongly depended on the reaction conditions. Syringaldehyde (13), vanillin (9), acetosyringone (14), syringone (6), guaiacol (5) and benzoic acids (11), were the major products, and various alkyl phenol (3) and alkyl benzene (2) was also produced (Table 3).

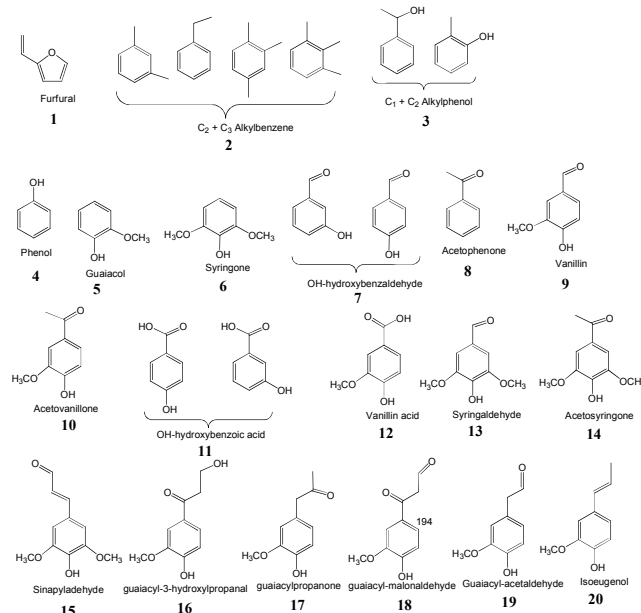


Fig 8: Monomeric products obtained from oxidative fragmentation of lignins.

The formation of alkyl benzene and alkyl phenol indicates clearly the demethoxylation of lignin polymer; which produced methanol, consecutive alkylations of the obtained phenol with methanol were considered to produce these compounds³⁸. Yan et al; 2017, reported also that the complete cleavage of aryl-O-bonds in phenols in the presence of ethanol over MoC_{1-x}/CuMgAlO₂ at 300°C⁴¹. With Fe₅₀-Co₅₀ catalyst for 4h of reaction in water, a total yield of identified aromatic compounds of 17.8% and 19.7% was observed at 200°C and 150°C, respectively (Exp.1 & 2), with a selectivity to syringaldehyde of 36.8% and 49.8%, respectively. Syringone (6), guaiacol (5), vanillin (9), acetosyringone (14) and alkylbenzene (2) were also produced with selectivity varying from 6 to 18% which depending in the temperature (Table 3). It is important to note that Fe₅₀-Co₅₀ catalyst exhibited high catalytic activity, and the aromatic monomers yield does not differ much for 150°C and 200°C. However, the selectivity towards aromatic compounds and particularly to syringaldehyde and vanillin depended on the temperature. For 150°C and 200°C, the selectivity to syringaldehyde and vanillin was much higher at 150°C than that obtained at 200°C. For instance, with Fe₅₀-Co₅₀ at 150°C, the syringaldehyde and vanillin represented about 50 wt% and 20%, respectively in the aromatic fraction. The amount of the aromatic lignin monomers increases also with increasing the reaction time, a total yield of

10.4% and 19.7% was observed for 2h and 4h, respectively at 200°C (Table 3, Exp.1 & 3), with a selectivity to syringaldehyde of about 35% for 2h and 4h, respectively. High selectivity of syringone (12%), guaïacol (15%), vanillin (15%) was also observed after 2h of reaction (Table 3, Exp.3) compared to only 7%, 6% and 12% obtained for 4h (Table 3, Exp.1). These results clearly indicate that aromatic lignin monomers increase with reaction time. However, at 200°C for 4h; the syringone, syringaldehyde and guaïacol will undergo an extensive demethoxylation to generate aromatic acids, ketones and alkylbenzene (Table 3). In all experiments of this study, prior to oxidation, the reactor was pressured up to 100 kPa with a mixture 10 % O₂ - 90% N₂. In order to point out the effect of the partial pressure of oxygen, oxidation tests were conducted under the same total pressure, but using oxygen-nitrogen mixtures with different concentrations. As shown by the results given in Table 3, the effect of the initial concentration of oxygen on both aromatic monomer yield and product distribution was considerable. Thus, the residual lignin (oligomers) decreased with increasing of oxygen partial pressure from 100 to 200 kPa (Table 3). In contrast, the total yield of aromatic products decreased from 178 to 133 mg/g lignin with an increase in oxygen partial pressure from 100 to 200 kPa. A high selectivity of vanillin (6%) acid and benzoic acids (10%) were observed at 200 kPa compared to 1% and 5%, respectively produced at 100 kPa. A further increase in oxygen partial pressure at 200 kPa, considerably reduced the amount of the aromatic oligomers, whereas the amount of non-aromatic products significantly increased. These results clearly indicate that, under an excess of oxygen, the initial oxidation products (aromatic species) were quickly oxidized into advanced degradation products. From these data presented in (Table 3) it is obvious that initially the aromatic aldehydes (vanillin and syringaldehyde) were selectively formed. Subsequently, the aldehydes reacted and the acids, phenols, ketones and alkyl phenols became the dominant products.

In contrast, the lignin conversion into monomers, and particularly into syringaldehyde (13) and vanillin (9), is substantially higher in reactions carried out in presence of Fe₅₀-Co₅₀ catalyst at 150°C or 200°C for 4h. For instance, the amount of aromatic products increases by a factor of 2.8 and 5.2 when the lignin oxidation was performed in the presence of 10 and 20 mg of Fe₅₀-Co₅₀, respectively. The positive effect of the catalyst on the vanillin and syringaldehyde yield is also noticeable. Thus, it was 9.6 and 17.8% (based on dry lignin) for 10 and 20 mg Fe₅₀-Co₅₀, respectively. It is important to note that the yield of the aromatic products reached 20% when the lignin was treated in the presence of 20 mg of catalyst at 150°C. We also note that only very low amount (3.4%) of aromatic compounds was identified without Fe₅₀-Co₅₀ catalyst at 200°C for 4h (Table 3). The small amount of aromatic molecules produced without catalysts were also observed in other studies⁴⁰. We are also studied the effect of organic solvent on the selectivity and yield of oxidative depolymerization of lignin (Table 3, Exp.6) by addition of 500 µl of methanol in the reaction. With methanol addition, a total yield of aromatic compounds of 16.6% was observed at 200°C (Table 3, Exp.6), with a high selectivity to alkylbenzene of 12%. These results confirm previous studies, which concluded the alkylation of phenol in the presence of methanol. This hypothesis confirmed by the reduction of char formation (lignin residual), which decreased to 44%, compared to 53% without methanol with similar conditions. The organic solvent such as methanol and ethanol act as capping agent and formaldehyde scavenger thereby suppressing char formation by reduction C-C linkage⁴². Yoshikawa et al. 2014 reported from the model studies that catechol methoxyphenol are converted to cresols and alkylbenzene over the iron oxide catalyst in the presence of 1-butanol⁴⁰.

Table 3: Amounts and selectivity of products resulted from the Organosolv lignin catalytic oxidation over Fe ₅₀ -Co ₅₀ catalyst							
Catalytic conditions	Exp.1	Exp.2	Exp.3	Exp.4	Exp.5	Exp.6	Exp.7
Cata. (mg)	20	20	20	20	10	20	0
Lignin (mg)	100	100	100	100	100	100	100
Temp. (°C)	200	150	200	200	200	200	200
Time (h)	4	4	2	4	4	4	4
O ₂ (KPa)	100	100	100	200	100	100	100
Solvent	Water	Water	Water	Water	Water	Water/Methanol	Water
Oligomers (lignin residual) (% w/w)	53.5	59.8	73.3	48.2	65.1	44.4	85.8
Non-identified molecules (% w/w)	28.7	20.6	14.3	38.5	22.3	39.0	10.8
Aromatic molecules (% w/w)	17.8	19.6	11.4	13.3	9.6	16.6	3.4
Selectivity (%)							
Alky benzene	7.73	7.00	4.24	7.72	3.59	12.04	2.50
Alkyl phenols	4.74	6.92	4.09	4.37	4.58	3.65	4.58
Acetophenone	2.02	2.05	0.15	1.04	0.11	2.15	1.20
Guaïacol	5.34	2.97	14.85	5.01	14.22	6.46	13.20
Syringone	7.41	1.38	11.45	0.69	9.04	8.18	7.96
OH-benzaldehyde	2.28	0.15	1.30	18.67	1.96	0.95	2.15
Vanillin	14.10	17.06	14.60	6.60	13.49	12.61	13.40
OH-benzoic acids	5.78	1.57	0.77	10.60	-	1.15	-
Acetovanillone	3.37	1.58	3.15	4.11	3.61	0.55	3.61
Vanillin acid	0.92	1.30	1.22	6.00	0.12	0.14	0.92
Syringaldehyde	35.83	49.77	34.48	30.53	32.63	38.84	35.63
Acetosyringone	7.58	3.80	6.40	3.59	7.96	6.16	5.26

Some comments may be drawn based on these results: (i) the lignin conversion into monomeric products decreases by increasing the temperature and decreasing the time; (ii) the sum of aromatic

compounds, as well as the aromatic aldehydes yield go through a maximum for a temperature of about 150°C in the presence of Fe₅₀-Co₅₀ catalyst; (iii) at 150°C the selectivity levels of syringaldehyde

ARTICLE

Journal Name

reached 50% (vi) The selectivity of alkyl benzene increased and reached 12% in the presence of methanol; (v) The recovery yield of aromatic compounds increases by increasing of catalyst charge; (iv) The selectivity of aromatic acids (benzoic and vanillin acids) increased for a oxygen pressure of 200KPa at 200°C.

Table 4: Catalyst recycling in the catalytic oxidation of lignin in water; 20mg of Fe ₅₀ -Co ₅₀ , 200 °C, 10 bar, 4 h			
	Run 1	Run 2	Run 3
Aromatic molecules (% w/w)	17.8	18.2	16.7
Selectivity			
Alky Benzene	7.73	5.83	7.88
Guaïacol	5.34	6.36	6.12
Syringone	7.41	8.50	7.86
Vanillin	14.10	14.80	13.65
Syringaldehyde	35.83	37.23	33.94

In order to obtain information on the stability of catalyst, as well as on the heterogeneous nature of the catalysis, the sample Fe₅₀-Co₅₀ was recycled in the oxidation of Organosolv lignin (150 °C, 100 kPa, 4h, 20 mg catalyst). The catalyst was recovered after reaction (see the experimental section), dried and then calcinated in airflow at 550°C for 4h. It was reused in a new experiment, under similar condition, using a fresh reaction mixture (Table 4).

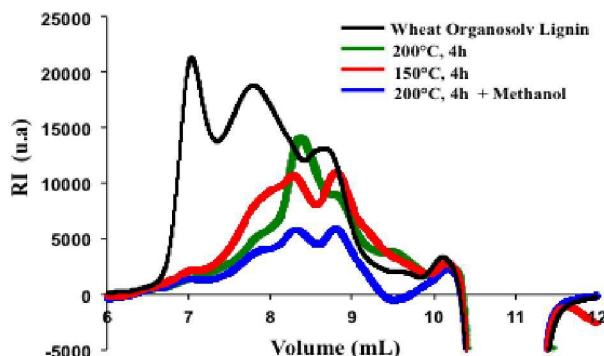


Fig.9: SEC chromatogram profiles of oligomers (residual lignin) formed from Organosolv lignin fragmentation under different conditions.

Beside the aromatic and non-aromatic molecular species, an important fraction (varying between 500 and 850 mg/g lignin) of oligomers (residual lignin) was obtained in the oxidation processes. In order to compare the initial and the residual lignins, the polymers were characterized by size-exclusion. As can be seen in Fig.9, major modifications were induced on the initial polymer during the catalytic oxidative depolymerization. The initial extracted wheat organosolv lignin has a molecular-average weight of 3180 g/mol and a wide molecular weight distribution. In contrast, the residual lignins have molecular weights lower than 1000 g/mol, which major peaks appearing at 600 and 300 g/mol. The level of polymer fragmentation depends on the oxidation conditions: the higher the oxidation severity (temperature, reaction time), the higher the fragmentation extent.

Conclusions

In this paper we propose an original method to convert lignin into aromatic monomers (mainly functionalized phenols) and water-soluble oligomers, using an aqueous neutral medium. Co₅₀-Fe₅₀

mixed oxide has been found to be excellent heterogeneous catalysts for the oxidative fragmentation of organosolv lignin in water, with diluted oxygen, under relatively low pressure. The product distribution strongly depended on the temperature, reaction time, oxygen partial pressure and catalyst amount. For instance, to obtain high yields in both monomeric compounds and aromatic aldehydes (syringaldehyde and vanillin) with a selectivity up to 60%, the following oxidation conditions should be employed: 100 mg of organosolv wheat straw lignin, 20 mg Co₅₀-Fe₅₀, temperature, 150°C, initial oxygen partial pressure, 100 kPa, reaction time, 4h.

References

1. J. Lora, in *Monomers, polymers and composites from renewable resources*, Elsevier, 2008, pp. 225-241.
2. M. Kleinert and T. Barth, *Chemical Engineering & Technology*, 2008, **31**, 736-745.
3. G. W. Huber, S. Iborra and A. Corma, *Chemical reviews*, 2006, **106**, 4044-4098.
4. T. Barth and M. Kleinert, *Chemical Engineering & Technology*, 2008, **31**, 773-781.
5. D. Stewart, *Industrial crops and products*, 2008, **27**, 202-207.
6. J. H. Lora and W. G. Glasser, *Journal of Polymers and the Environment*, 2002, **10**, 39-48.
7. C. Amen-Chen, H. Pakdel and C. Roy, *Bioresource Technology*, 2001, **79**, 277-299.
8. V. Tarabanko, D. Petukhov and G. Selyutin, *Kinetics and Catalysis*, 2004, **45**, 569-577.
9. M. B. Hocking, *Journal of chemical education*, 1997, **74**, 1055.
10. H. Deng, L. Lin, Y. Sun, C. Pang, J. Zhuang, P. Ouyang, Z. Li and S. Liu, *Catalysis Letters*, 2008, **126**, 106-111.
11. C.-L. Chen, in *Methods in lignin chemistry*, Springer, 1992, pp. 301-321.
12. J. Villar, A. Caperos and F. Garcia-Ochoa, *Wood Science and Technology*, 2001, **35**, 245-255.
13. T. Voith and P. Rudolf von Rohr, *ChemSusChem*, 2008, **1**, 763-769.
14. A. R. Gaspar, J. A. Gamelas, D. V. Evtuguin and C. P. Neto, *Green Chemistry*, 2007, **9**, 717-730.
15. J. Gamelas, A. Pontes, D. Evtuguin, A. Xavier and A. Esculcas, *Biochemical engineering journal*, 2007, **33**, 141-147.
16. A. P. Tavares, J. A. Gamelas, A. R. Gaspar, D. V. Evtuguin and A. M. Xavier, *Catalysis Communications*, 2004, **5**, 485-489.
17. J. Gamelas, A. Gaspar, D. Evtuguin and C. P. Neto, *Applied Catalysis A: General*, 2005, **295**, 134-141.
18. A. R. Gonçalves and U. Schuchardt, *Applied biochemistry and Biotechnology*, 1999, **77**, 127-132.
19. G. A. A. Labat and A. R. Gonçalves, *Applied biochemistry and biotechnology*, 2008, **148**, 151-161.
20. W. Partenheimer, *Advanced Synthesis & Catalysis*, 2009, **351**, 456-466.
21. H. Deng, L. Lin, Y. Sun, C. Pang, J. Zhuang, P. Ouyang, Z. Li and S. Liu, *Catalysis letters*, 2008, **126**, 106.
22. C. Crestini, P. Pro, V. Neri and R. Saladino, *Bioorganic & medicinal chemistry*, 2005, **13**, 2569-2578.
23. C. Crestini, M. C. Caponi, D. S. Argyropoulos and R. Saladino, *Bioorganic & medicinal chemistry*, 2006, **14**, 5292-5302.
24. C. Crestini, R. Saladino, P. Tagliatesta and T. Boschi, *Bioorganic & medicinal chemistry*, 1999, **7**, 1897-1905.
25. C. Crestini, A. Pastorini and P. Tagliatesta, *Journal of Molecular Catalysis A: Chemical*, 2004, **208**, 195-202.
26. C. Crestini, A. Pastorini and P. Tagliatesta, *European Journal of Inorganic Chemistry*, 2004, **2004**, 4477-4483.
27. H. Q. Lam, Y. Le Bigot, M. Delmas and G. Avignon, *Industrial Crops and Products*, 2001, **14**, 139-144.
28. G. Labat, J. L. Seris and B. Meunier, *Angewandte Chemie International Edition*, 1990, **29**, 1471-1473.

Journal Name

ARTICLE

29. A. Abad, C. Almela, A. Corma, H. García, *Tetrahedron*, 2006, **62**, 6666-6672.
30. M. P. Woods, B. Mirkelamoglu, U.S. Ozkan, *J. Phys. Chem. C*, 2009, **113**, 10112-10119.
31. S. Constant, A. Barakat, M. Robitzer, F. Di Renzo, C. Dumas and F. Quignard, *Bioresource technology*, 2016, **216**, 737-743.
32. A. Barakat, B. Chabbert and B. Cathala, *Phytochemistry*, 2007, **68**, 2118-2125.
33. N. Aust, M. Parth and K. Lederer, *International Journal of Polymer Analysis and Characterization*, 2001, **6**, 245-260.
34. A. S. Bhatt, D. K. Bhat, C.-w. Tai and M. S. Santosh, *Materials Chemistry and Physics*, 2011, **125**, 347-350.
35. R. D. Shannon, *Acta crystallographica section A: crystal physics, diffraction, theoretical and general crystallography*, 1976, **32**, 751-767.
36. F. Giovannelli, V. Marsteau, M. Zaghrioui, C. Autret and F. Delorme, *Advanced Powder Technology*, 2017, **28**, 1325-1331.
37. Z. L. Wang and X. Feng, *The Journal of Physical Chemistry B*, 2003, **107**, 13563-13566.
38. A. López-Ortega, E. Lottini, C. d. J. Fernandez and C. Sangregorio, *Chemistry of Materials*, 2015, **27**, 4048-4056.
39. C. Xu, R. A. D. Arancon, J. Labidi and R. Luque, *Chemical Society Reviews*, 2014, **43**, 7485-7500.
40. T. Yoshikawa, T. Yagi, S. Shinohara, T. Fukunaga, Y. Nakasaka, T. Tago and T. Masuda, *Fuel processing technology*, 2013, **108**, 69-75.
41. F. Yan, R. Ma, X. Ma, K. Cui, K. Wu, M. Chen and Y. Li, *Applied Catalysis B: Environmental*, 2017, **202**, 305-313.
42. X. Huang, C. Atay, J. Zhu, S. W. Palstra, T. I. Korányi, M. D. Boot and E. J. Hensen, *ACS sustainable chemistry & engineering*, 2017, **5**, 10864-10874.

Conflicts of interest

There are no conflicts to declare.

Acknowledgements

This study was financially supported by the University Mohamed VI Polytechnic (UM6P) of Benguerir and INRA SupAgro Montpellier.

CoFeO mixed oxide an efficient catalyst for lignin depolymerization in water to functional phenols

